

Optical and acoustic phonon modes in self-organized Ge quantum dot superlattices

J. L. Liu,^{a)} G. Jin, Y. S. Tang, Y. H. Luo, and K. L. Wang

Device Research Laboratory, Department of Electrical Engineering, University of California at Los Angeles, Los Angeles, California 90095-1594

D. P. Yu

Electron Microscopy Laboratory, Peking University, Beijing 100871, People's Republic of China

(Received 22 September 1999; accepted for publication 3 December 1999)

Raman scattering measurements were carried out in self-organized Ge quantum dot superlattices. The samples consisted of 25 periods of Ge quantum dots with different dot sizes sandwiched by 20 nm Si spacers, and were grown using solid-source molecular-beam epitaxy. Optical phonon modes were found to be around 300 cm^{-1} , and a dependence of the Raman peak frequency on the size of dots was evidenced in good agreement with a prediction based on phonon confinement and strain effects. Acoustic phonons related to the Ge quantum dots have also been observed. © 2000 American Institute of Physics. [S0003-6951(00)03305-2]

In recent years, considerable attention has been paid to self-organized Ge quantum dots both for fundamental physics studies and potential applications. Among those studies, a number of attempts were devoted to understanding the dot formation mechanism.¹ Meanwhile, interband² and intersubband³ properties of Ge quantum dots have been studied for the development of novel quantum dot lasers and detectors. In addition, the well-arranged dot arrays were studied for possible applications in information processing.⁴ Recently, we have shown that a Ge quantum dot system could have very small thermal conductivity and thus a high figure of merit for potential applications in implementing solid state refrigerator.⁵ For this purpose, understanding the vibrational phonon processes in Ge quantum dots was indispensable since phonons are very important for heat transport, particularly in semiconductors. Indeed, a great deal of effort has been invested in studying the phonon transport processes due to strain effects and the change of alloy composition in single-layered Ge dots.⁶ In contrast, little⁷ has been done on multilayered dot superlattices. In this letter, we report the study of optical and acoustic phonons in Ge quantum dot superlattices by Raman scattering measurements.

Three samples, labeled A, B, and C, were grown by solid source molecular beam epitaxy on Si(100) substrates kept at a temperature of $600\text{ }^{\circ}\text{C}$ and with growth rates of 1 and 0.2 \AA/s for Si and Ge, respectively. All of these samples consisted of 100 nm Si buffer layers, followed by 25 bilayers, in which Ge layers were separated by 20-nm-thick Si spacer layers. The only difference among these samples is the different amounts of Ge deposition, yielding to different dot sizes. The thin foils destined for microstructure study were prepared using a cross-sectional procedure combined with ion milling. A Hitachi-9000NAR high-resolution electron microscope (HREM) with point-to-point resolution of 0.18 nm was employed for the microstructure analysis. Figure 1 shows two cross-sectional HREM images of sample C. The

bright contrast regions in Fig. 1(a) are the Si spacer layers, while dark stripes are Ge wetting layers. In addition, many small dark features along the Ge wetting layers are from Ge quantum dots. Indeed, Fig. 1(b) shows the HREM image of

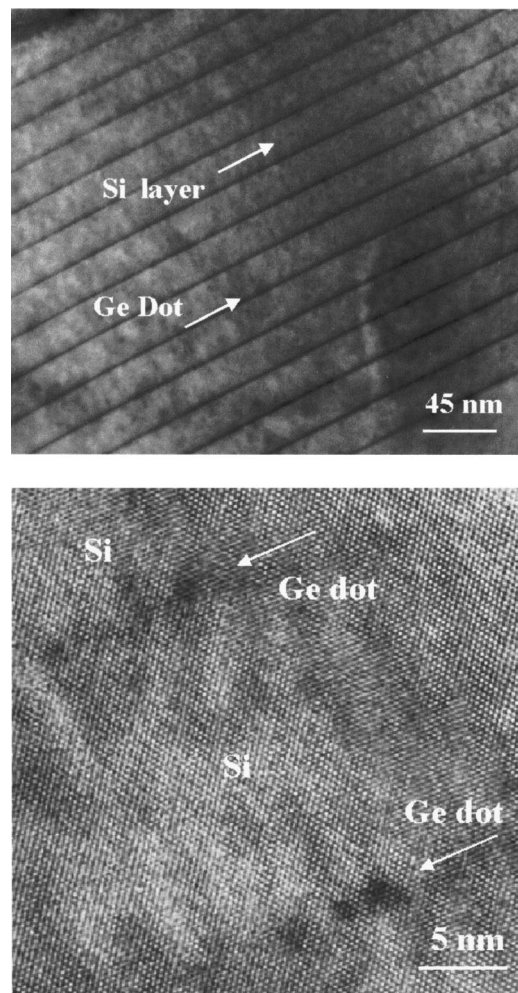


FIG. 1. (a) Low- and (b) high-resolution cross-sectional HREM images of sample C. The Ge quantum dot superlattice is evident.

^{a)}Electronic mail: jliu@ee.ucla.edu

TABLE I. Structural data of the samples used in this experiment.

	Dot height (Å)	Density (cm ⁻²)	Nonuniformity
Sample A	0 ^a
Sample B	15	1.6×10 ⁸	8%
Sample C	20	2.8×10 ⁸	7%

^aNo dots but wetting layers.

small Ge quantum dots with a typical height of 20 Å. Table I summarizes the structural properties of these samples. The amount of Ge in each Ge layer of sample A was controlled such that there was no visible dot formation but Ge wetting layers. As more Ge was deposited in samples B and C, it was measured that the height of the Ge dots was 15 and 20 Å for samples B and C, respectively. The dot densities and uniformities shown in Table I were obtained by atomic force microscopy scanning over the surfaces after the first Ge layers growth, indicating some differences between samples B and C.

Raman scattering measurements were performed with a Renishaw Raman Imaging 2000 microscope at room temperature. All spectra were excited by the 514 nm line of an Ar⁺ ion laser and recorded with a Si charge-coupled device camera. Figure 2 shows the Raman spectra of the samples. The spectra were obtained in the 001(100,100)00 $\bar{1}$ back-scattering configuration with the same data accumulation time. As seen from Fig. 2, the Ge-Ge optical modes can be clearly found at 296.5 and 298.2 cm⁻¹ for samples B and C, respectively. For sample A, however, the Ge-Ge mode is too weak to be seen. First, it is important to distinguish these Ge-Ge modes of samples B and C from the second order transverse acoustic phonon modes for Si, which are typically around 303 cm⁻¹ under proper configurations.⁸ In fact, these Raman lines are asymmetric with a tail at the low-frequency side. Moreover, as the Ge dot size decreases the peak broadens and softens. This phenomenon, which is typically observed in the Ge nanocrystals,⁶ is due to phonon confinement effects.⁹ Furthermore, we argue that the Ge-Ge modes from samples B and C are mainly from their Ge dots rather than their Ge wetting layers. This is because in the 001(100,100)00 $\bar{1}$ backscattering configuration, the signals from the two-dimensional Ge wetting layers are forbidden according to the selection rules.¹⁰ The point can also be concluded by comparing the relatively strong Ge-Ge modes in

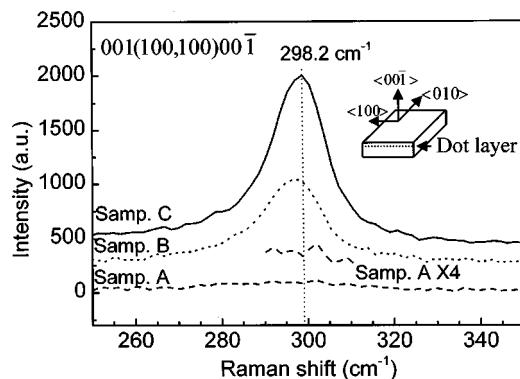


FIG. 2. Raman spectra of the samples indicating different Ge-Ge optical modes for different samples.

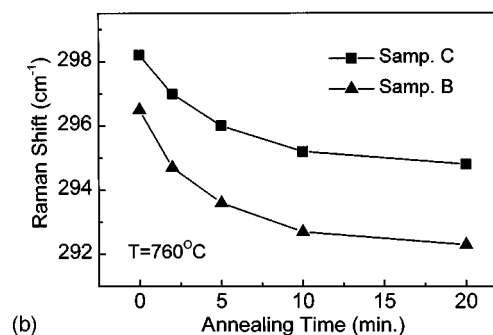
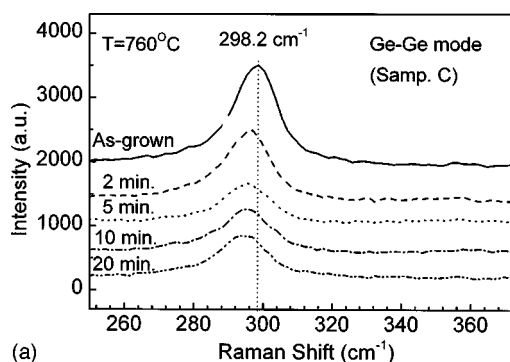


FIG. 3. (a) Raman spectra of sample C annealed at 760 °C for different times and (b) annealing time dependence of the Raman shift for samples B and C. The Ge-Ge optical mode frequency for both samples decreases as the annealing time increases.

samples B and C with a very weak signal from sample A. It is well known that the first order Ge-Ge optical mode frequency for bulk Ge is at 300 cm⁻¹, but the Ge-Ge mode frequency of Ge nanocrystals can be changed by phonon confinement and strain effects: compressive strain leads to an upward shift of the Ge-Ge mode, while phonon confinement leads to a downward shift. Here, the additional phonon confinement effects in the dots of samples B and C compensate with the contribution from the compressive strain and lead to the downward shift of the Ge-Ge mode. Moreover, the smaller the dots (sample B) the stronger the phonon confinement effects, and thus, the lower the Ge-Ge optical mode frequency (296.5 cm⁻¹, compared with 298.2 cm⁻¹ of sample C).

Phonon confinement effects in the Ge quantum dots can be further confirmed by performing annealing experiments. Figure 3(a) shows a series of Raman spectra for sample C. All pieces were annealed at 760 °C for different times. The Ge-Ge Raman line broadens and shifts to lower frequencies as the annealing time increases. This phenomenon was also observed when annealing sample B. Figure 3(b) shows the annealing time dependence of the Raman shift for samples B and C. After a 20 min annealing, the Ge-Ge optical mode shifted downward by as much as 3.8 and 3.4 cm⁻¹ for samples B and C, respectively. The compressive strain relaxes with increasing annealing time, and thus, the phonon confinement effects become relatively more important, which causes the observed peak shift.

Figure 4 shows Raman spectra for the three samples and an identical substrate obtained in the 001(110,110)00 $\bar{1}$ back-scattering configuration. As clearly seen from Fig. 4, sample C has four orders of acoustic phonons, which are indicated by arrows at 70, 94.5, 118.2, and 137.6 cm⁻¹. Sample B has

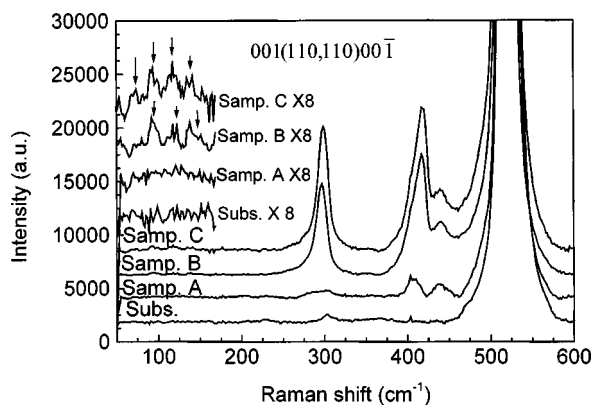


FIG. 4. Raman spectra of the samples and an identical substrate, showing clear acoustic phonon peaks only from samples B and C.

three at 95.4, 120.4, and 145.2 cm^{-1} . No observable acoustic phonons are found for sample A and substrate. It is found that the first order acoustic phonon frequency increases with the decrease of the dot size, which is quite similar to that in the quantum well case,¹¹ and is also predicted in Si nanocrystals.¹² Obviously, these acoustic phonons in samples B and C are related to the Ge quantum dot superlattices. However, more studies, such as resonance Raman, are needed to verify whether these acoustic phonons are confined in the Ge dots or scattered by them.

In summary, we have reported Raman scattering studies on self-organized Ge quantum dot superlattices. Optical phonon confinement was evidenced in the Ge dots and the phonon frequency was found to change with the dot size and strain effects. Acoustic phonons related to the Ge quantum dot superlattices were observed.

This work was supported by a US DoD/ONR MURI project on thermoelectrics (Dr. John Pazik).

- ¹J. Tersoff, C. Teichert, and M. G. Lagally, *Phys. Rev. Lett.* **76**, 1675 (1996); H. T. Dobbs, D. D. Vvedensky, A. Zangwill, J. Johansson, N. Carlsson, and W. Seifert, *ibid.* **79**, 897 (1997); O. G. Schmidt, O. Kienzle, Y. Hao, K. Eberl, and F. Ernst, *Appl. Phys. Lett.* **74**, 1272 (1999).
- ²C. S. Peng, Q. Huang, W. Q. Cheng, J. M. Zhou, Y. H. Zhang, T. T. Sheng, and C. H. Tung, *Phys. Rev. B* **57**, 8805 (1998); E. S. Kim, N. Usami, and Y. Shiraki, *Appl. Phys. Lett.* **72**, 1617 (1998); M. Goryll, L. Vescan, and H. Luth, *Thin Solid Films* **336**, 244 (1998).
- ³P. Boucaud, V. Le Thanh, S. Sauvage, D. Debarre, and D. Bouchier, *Appl. Phys. Lett.* **74**, 401 (1999); J. L. Liu, W. G. Wu, A. Balandin, G. L. Jin, and K. L. Wang, *ibid.* **74**, 185 (1999).
- ⁴A. Balandin and K. L. Wang, *Superlattices Microstruct.* **25**, 509 (1999); C. S. Lent, P. D. Tougaw, W. Porod, and G. H. Bernstein, *Nanotechnology* **4**, 19 (1993); G. Jin, J. L. Liu, S. G. Thomas, Y. H. Luo, K. L. Wang, and Bich-Yen Nguyen, *Appl. Phys. Lett.* **75**, 1745 (1999).
- ⁵K. L. Wang, J. L. Liu, A. Balandin, and A. Khitun (unpublished).
- ⁶J. Groenen, R. Carles, S. Christiansen, M. Albrecht, W. Dorsch, and H. P. Strunk, *Appl. Phys. Lett.* **71**, 3856 (1997); C. E. Bottani, C. Mantini, P. Milani, M. Manfredini, A. Stella, P. Tognini, P. Cheyssac, and R. Kofman, *ibid.* **69**, 2409 (1996); P. D. Persans, P. W. Deelman, K. L. Stokes, L. J. Schowalter, A. Byrne, and T. Thundat, *ibid.* **70**, 472 (1997).
- ⁷J. L. Liu, Y. S. Tang, K. L. Wang, T. Radetic, and R. Gronsky, *Appl. Phys. Lett.* **74**, 1863 (1999).
- ⁸K. Uchinokura, T. Sekine, and E. Matsuura, *J. Phys. Chem. Solids* **35**, 17 (1974).
- ⁹P. M. Fouchet and J. H. Cambell, *Crit. Rev. Solid State Mater. Sci.* **14**, S79 (1988); J. Gonzalez-Hernandez, G. H. Azerbayejani, R. Tsu, and F. H. Pollak, *Appl. Phys. Lett.* **47**, 1350 (1985).
- ¹⁰R. Schorer, G. Abstreiter, S. De Gironcoli, E. Molinari, H. Kibbel, and H. Presting, *Phys. Rev. B* **49**, 5406 (1994).
- ¹¹M. I. Alonso, F. Cerdeira, D. Niles, M. Cardona, E. Kasper, and H. Kibbel, *J. Appl. Phys.* **66**, 5645 (1989); C. Colvard, T. A. Gant, M. V. Klein, R. Merlin, R. Fischer, H. Morkoc, and A. C. Gossard, *Phys. Rev. B* **31**, 2080 (1985).
- ¹²J. Zi, K. Zhang, and X. Xie, *Phys. Rev. B* **58**, 6712 (1998); M. Fujii, Y. Kanzawa, S. Hayashi, and K. Yamamoto, *Phys. Rev. B* **54**, 8373 (1996).